

Mechanism of Slow Relaxation due to Screening Effect in a Frustrated System

Shu TANAKA* and Seiji MIYASHITA^{1,2†}

Institute for Solid State Physics, University of Tokyo, 5-1-5 Kashiwanoha, Kashiwa-shi, Chiba 277-8581, Japan

¹ *Department of Physics, University of Tokyo, 7-3-1 Hongo, Bunkyo-ku, Tokyo 113-0033, Japan*

² *CREST, JST, 4-1-8, Honcho Kawaguchi, Saitama 332-0012, Japan*

We study a slow relaxation process in a frustrated spin system in which a type of screening effect due to a frustrated environment plays an important role. This screening effect is attributed to the highly degenerate configurations of the frustrated environment. This slow relaxation is due to an entropy effect and is different from those due to the energy barrier observed in systems such as random ferromagnets. In the present system, even if there is no energy gap, the slow relaxation still takes place. Thus, we call this phenomenon “entropic slowing down”. Here, we study the mechanism of entropic slowing down quantitatively in an Ising spin model with the so-called decorated bonds. The spins included in decorated bonds (decoration spins) cause a peculiar density of states, which causes an entropy-induced screening effect. We analytically estimate the time scale of the system that increases exponentially with the number of decoration spins. We demonstrate the scaling of relaxation processes using the time scale at all temperatures including the critical point.

KEYWORDS: slow relaxation, Ising spin system, frustration, decorated bond system, entropy effect

1. Introduction

The mechanisms of slow relaxation in strongly interacting systems have been studied over the past several decades. One of them is the critical slowing down.¹⁻⁴ When the correlation of an order parameter develops near a critical point, the system shows a slow relaxation. If the interactions of a system are nonuniform, as in the diluted ferromagnetic model, the model shows a slow relaxation even in the off-critical region. After quenching from a random state the order develops locally, but the domain walls between them are pinned in regions of relatively weak interaction. This pinning causes a very slow relaxation that may be called a frozen state.⁵⁻⁷ Furthermore, when the system has frustration, as in spin glass, the frustration causes a random distribution of effective interactions and the relaxation also becomes slow.⁸⁻¹² In a frustrated system, many competing configurations are degenerate, and the system has a peculiar density of state that causes a temperature-dependent ordering structure,¹³⁻¹⁵ and

*E-mail address: shu-t@issp.u-tokyo.ac.jp

†E-mail address: miya@spin.phys.s.u-tokyo.ac.jp

even reentrant phase transitions.^{13,16,17}

Recently, it has been found that an extremely slow relaxation takes place in a decorated lattice.¹³ The static properties of the decoration lattice are described by an effective coupling due to a decorated bond, and are the same as those of a regular lattice that has a coupling constant, but the dynamics of the systems are very different because the motion of decoration spins prevents the smooth evolution of ordering. This screening effect comes from the distribution of degrees of freedom of decoration spins, and we call it “entropic slowing down.” This slow relaxation occurs even if there is no energy barrier.

The purpose of the present study is to clarify the feature of the entropic slowing down, and to quantitatively analyze the time scale of the slowing down. Using the time scale, we demonstrate a scaling analysis of the relaxation processes obtained by a Monte Carlo simulation with the Glauber dynamics.¹⁸

Using the present slow-relaxation mechanism, we propose a new memory system that we call the “spin blackboard”. In such a system, we can memorize all configurations at low temperatures and erase them by increasing the temperature.

In §2, we first introduce the model and present its equilibrium and dynamical properties. We present the probability distribution of the frustrated local structure in §3. The effective time scale can be calculated analytically. In §4, we study the relaxation of magnetization on a square lattice system by Monte Carlo simulation and perform the scaling plot using the effective time obtained in §3. We provide a summary of this study in §5. In Appendix, we analyze the flip probability by another energy unit.

2. Model and Equilibrium Properties

We have studied the ordering process of a decorated bond system. A decorated bond system consists of the so-called skeleton lattice, consisting of “system spins” and the decorated bonds between them. In each decorated bond, the system spins are connected by a bunch of paths that are mutually frustrated, as depicted in Fig. 1(a). To study the entropy effects on relaxation phenomena, we introduce the two-dimensional square lattice Ising spin system with decorated bonds depicted in Fig. 1(b). In Fig. 1(a), the frustrated local structure of the decorated bond unit is depicted. The circles denote “system spins” which form the square lattice as depicted in Fig. 1(b). The triangles denote “decoration spins” $\{s_i\}$, that are placed in the structure of a decorated bond. There are N_d decoration spins between a nearest-neighbor pair of the system spins σ_1 and σ_2 . We adopt the following structure of the decorated bond. We set half of the paths in a decorated bond in a ferromagnetic way, *i.e.*, by two ferromagnetic bonds (solid lines) with a decoration spin between them. The other half of the paths are set in an antiferromagnetic way with ferromagnetic and antiferromagnetic bonds (dotted lines) with a decoration spin between them. The magnitudes of these bonds are set to be the same (J). As we will show below, the contributions of the ferromagnetic and antiferromagnetic paths

cancel out, and the effective interaction between the system spins due to the N_d paths is zero.

In order to study the phase transition, in addition, we set the extra bond (a wavy line) that causes the interaction between the system spins to be nonzero. We impose the periodic boundary condition on the lattice depicted in Fig. 1(b).

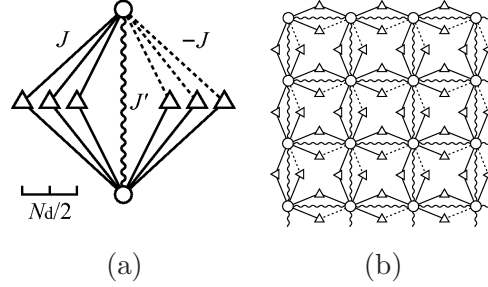


Fig. 1. (a) Frustrated decorated bond unit. The circles and triangles denote the system and decoration spins, respectively. The solid, dotted, and wavy lines denote the magnetic interactions of J , $-J$, and J' , respectively. (b) Two-dimensional square lattice with decorated bonds in the case of $N_d = 2$.

The Hamiltonian of a decorated bond depicted in Fig. 1(a) is

$$\mathcal{H} = -J'\sigma_1\sigma_2 - J \sum_{i=1}^{N_d/2} s_i (\sigma_1 + \sigma_2) - J \sum_{i=N_d/2+1}^{N_d} s_i (-\sigma_1 + \sigma_2), \quad (1)$$

where σ_1 and σ_2 denotes the system spins and s_i ($i = 1, \dots, N_d$) denote the decoration spins. The solid, dashed, and wavy lines in Fig. 1 denote the magnetic interactions of J , $-J$, and J' , respectively. Hereafter, we take J as the unit of energy. The effective coupling K_{eff} between the system spins σ_1 and σ_2 at a temperature $T = 1/\beta$ is defined by tracing out the decoration spins $\{s_i\}$:

$$\sum_{\{s_i=\pm 1\}} e^{-\beta\mathcal{H}} = Ae^{-\beta\mathcal{H}_{\text{eff}}} = Ae^{-K_{\text{eff}}\sigma_1\sigma_2}, \quad (2)$$

where

$$A = (4 \cosh 2\beta J)^{N_d/2}, \quad (3)$$

$$K_{\text{eff}} = \beta J'. \quad (4)$$

Since the contributions of the left and right-half paths in Fig. 1(a) cancel out, the effective coupling of this system comes only from J' . The relation between the correlation function $\langle\sigma_1\sigma_2\rangle$ and the effective coupling K_{eff} is given by

$$\langle\sigma_1\sigma_2\rangle = \tanh K_{\text{eff}}. \quad (5)$$

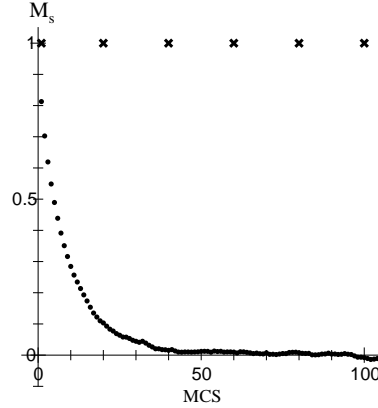


Fig. 2. Relaxation process of the system magnetization on a square lattice system with decorated bonds, where the number of system spins is $N = 20^2$, at $T = 3$, which is above the critical temperature. The circles indicate the relaxation process of the regular system ($N_d = 0$) and the crosses represent that of the decorated bond system of $N_d = 200$.

If $J' > 0$, $\langle \sigma_1 \sigma_2 \rangle$ is positive. If the effective coupling K_{eff} is larger than the critical value K_c , the system spins have a ferromagnetic long-range order in the equilibrium state. Here, we consider the case of $J' = 1$.

Next, we consider the square lattice system with decorated bonds depicted in Fig. 1(b). We perform a single spin flip of the heat bath method of Monte Carlo simulation to consider the dynamical aspects in the system. We study a relaxation process of the system magnetization

$$M_s = \frac{1}{N} \sum_i^N \sigma_i, \quad (6)$$

from an ordered state in which all the spins are aligned in the same direction. Here, we set the temperature in the paramagnetic region $T = 3$, *i.e.*, $K_{\text{eff}} = 1/3 < K_c = [\frac{1}{2} \log(1 + \sqrt{2})]^{-1} = (2.27 \dots)^{-1}$. At this temperature, we expect a fast relaxation to $M_s = 0$ in the regular lattice ($N_d = 0$). However, in the decoration bond system ($N_d > 1$), we expect the effect of the frustrated configuration although the thermodynamic properties, such as the correlation functions of the system spin, are the same in both systems.

We performed a Monte Carlo simulation of the square lattice system depicted in Fig. 1(b) with $N = 20^2$ system spins. In Fig. 2, we compare the relaxations of M_s in the regular and decorated lattices. The data are obtained by taking the average of one thousand samples. The magnetization in the regular lattice relaxes with a relaxation time $\tau_{\text{reg}} \simeq 10$ Monte Carlo Step (MCS) we see no relaxation in the decorated bond system in this time scale. In the next section we will focus on the microscopic mechanism of this slow relaxation in decorated bond systems.

3. Probability Distribution of Frustrated Local Structure

In the previous section, we showed an example of the entropic slowing down by Monte Carlo simulation. A large number of degenerate states cause such a slowing down. In this section, we analyze this slow relaxation from the viewpoint of the probability distribution of the decoration spins depicted in Fig. 1(a). We determine the number of states for a fixed local configuration of system spins. We depict “the parallel state” of system spins, *i.e.*, $(\sigma_1, \sigma_2) = (+, +)$, and “the antiparallel state”, *i.e.*, $(\sigma_1, \sigma_2) = (+, -)$ in Figs. 3(a) and (b), respectively, where the black, white, and gray symbols denote the sites with $+$, $-$, and 0 internal fields, respectively. We denote the number of $+$ decoration spins in the ferromagnetic paths by m , and that in the antiferromagnetic paths by n . The energy of the parallel state is given by

$$E_{++}^{(N_d)}(m, n) = (N_d - 4m)J - J'. \quad (7)$$

The energy of the parallel state does not depend on n , because the energy of each antiferromagnetic path does not depend on the states of decoration spins. In the same way, the energy of the antiparallel state is given by

$$E_{+-}^{(N_d)}(m, n) = (-N_d + 4n)J + J', \quad (8)$$

which is independent of m . Note that the following relations are satisfied:

$$E_{++}^{(N_d)}(m, n) = E_{--}^{(N_d)}\left(\frac{N_d}{2} - m, n\right), \quad (9)$$

$$E_{+-}^{(N_d)}(m, n) = E_{-+}^{(N_d)}\left(m, \frac{N_d}{2} - n\right). \quad (10)$$

Because the maximum values of m and n are $N_d/2$, the ground state energy of the parallel state is given by

$$E_{++}^{(N_d)}\left(\frac{N_d}{2}, n\right) = -N_d J - J' \quad (11)$$

and the number of degeneracies is $2^{N_d/2}$. Similarly, the minimum energy of the antiparallel state is given by

$$E_{+-}^{(N_d)}(m, 0) = -N_d J + J'. \quad (12)$$

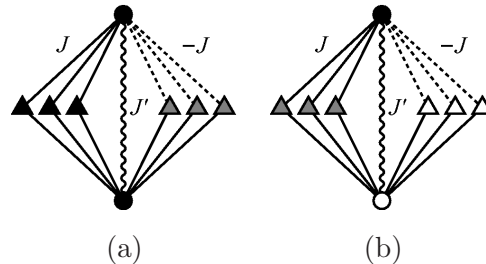


Fig. 3. Black, white, and gray symbols denote the sites with $+$, $-$, and 0 internal fields, respectively. (a) Parallel system spin case and (b) antiparallel system spin case.

The lowest energy of the antiparallel state ($n = 0$) is higher than that of the parallel state by $2J'$.

We consider the probability distribution of the decoration spins at a temperature T . First, we consider the parallel case. The probability of m up spins in the $N_d/2$ ferromagnetic paths is given by

$$Q_{++}^{(N_d)}(m) = \frac{e^{-\beta J N_d}}{(2 \cosh 2\beta J)^{N_d/2}} \binom{N_d/2}{m} e^{4\beta J m}, \quad (13)$$

and the probability of n up spins in the antiferromagnetic paths is given by

$$R_{++}^{(N_d)}(n) = \binom{N_d/2}{n} \left(\frac{1}{2}\right)^{N_d/2}. \quad (14)$$

On the other hand, if the system is in the antiparallel case, the probability of m up spins in the ferromagnetic paths is given by

$$Q_{+-}^{(N_d)}(m) = \binom{N_d/2}{m} \left(\frac{1}{2}\right)^{N_d/2}, \quad (15)$$

which is equal to $R_{++}^{(N_d)}(m)$. The probability of n up spins in the antiferromagnetic paths is given by

$$R_{+-}^{(N_d)}(n) = \frac{e^{\beta J N_d}}{(2 \cosh 2\beta J)^{N_d/2}} \binom{N_d/2}{n} e^{-4\beta J n}, \quad (16)$$

which is equal to $Q_{--}^{(N_d)}(m)$. From the symmetry, the following relations hold:

$$Q_{++}^{(N_d)}(m) = Q_{--}^{(N_d)}\left(\frac{N_d}{2} - m\right), \quad (17)$$

$$R_{++}^{(N_d)}(n) = R_{--}^{(N_d)}(n), \quad (18)$$

$$Q_{+-}^{(N_d)}(m) = Q_{-+}^{(N_d)}(m), \quad (19)$$

$$R_{+-}^{(N_d)}(n) = R_{-+}^{(N_d)}\left(\frac{N_d}{2} - n\right). \quad (20)$$

Because $R_{++}^{(N_d)}(n)$ and $Q_{+-}^{(N_d)}(m)$ are simple binary distributions, they are independent of temperature. The distributions become sharp when the number of decorated spins increases. On the other hand, $Q_{++}^{(N_d)}(m)$ and $R_{+-}^{(N_d)}(n)$ depend on temperature. At high temperatures, they are maximum at $N_d/4$ owing to the entropy effect. At low temperatures, they are maximum at nearly $N_d/2$ and 0, respectively, because they are energetically favored states for the distributions.

The probability of the total distributions of the parallel and antiparallel states are given by

$$P_{++}^{(N_d)}(m, n) = Q_{++}^{(N_d)}(m) R_{++}^{(N_d)}(n), \quad (21)$$

$$P_{+-}^{(N_d)}(m, n) = Q_{+-}^{(N_d)}(m) R_{+-}^{(N_d)}(n), \quad (22)$$

respectively. Figure 4 shows color maps of the probability distributions $P_{++}^{(N_d)}(m, n)$, $P_{+-}^{(N_d)}(m, n)$, and their overlap $P_{++}^{(N_d)}(m, n)P_{+-}^{(N_d)}(m, n)$ as a function of the numbers of + decoration spins (m and n) for $T = 100$, $T = 10$, and $T = 1$ in the case of $N_d = 200$.

The probability function is a binary distribution of m and n at high temperatures, *e.g.*, $T = 100$, where the overlap is large (left columns in Fig. 4). As temperature decreases, the probability distributions split from the center point and the overlap decreases (center columns of Fig. 4). At low temperatures, *e.g.*, $T = 1$, the peaks of the probability distributions move to the edges because decoration spins with nonfrustrated paths polarize, and the overlap becomes very small (right columns in Fig. 4). Therefore, the transition probability between the parallel and antiparallel state becomes very small at low temperatures.

Thus, if the system is initially in the antiparallel state, there is a very small probability of transition to the parallel state, and the time scale of the evolution of the configuration becomes very long. Therefore, the system cannot reach the equilibrium state within a short time.

We denote the probabilities as \mathcal{P}_{++} and \mathcal{P}_{+-} for the parallel and antiparallel configurations of the system spin obtained by tracing out the degree of freedom of decoration spins. They are given by

$$\mathcal{P}_{++}^{(N_d)} = \sum_{m=0}^{N_d/2} \sum_{n=0}^{N_d/2} Q_{++}^{(N_d)}(m) R_{++}^{(N_d)}(n) \frac{e^{\beta J'}}{e^{\beta J'} + e^{-\beta J'}} = \frac{e^{\beta J'}}{e^{\beta J'} + e^{-\beta J'}}, \quad (23)$$

$$\mathcal{P}_{+-}^{(N_d)} = \sum_{m=0}^{N_d/2} \sum_{n=0}^{N_d/2} Q_{+-}^{(N_d)}(m) R_{+-}^{(N_d)}(n) \frac{e^{-\beta J'}}{e^{\beta J'} + e^{-\beta J'}} = \frac{e^{-\beta J'}}{e^{\beta J'} + e^{-\beta J'}}, \quad (24)$$

and they agree with the thermal equilibrium probabilities.

To estimate the effective relaxation time of this system, we calculate the flip probability of the central spin in the configuration shown in Fig. 5. This spin is surrounded by two up system spins and two down system spins. Suppose we consider a regular spin system, *i.e.*, $N_d = 0$. The internal fields from four neighbor system spins cancel out, and the energy difference between the up and down states of the central spin is zero. Thus, we call the central spin a “free spin”. The transition probability of the center spin is 1/2 in the Glauber dynamics.¹⁸ However, as we will show below, in decorated bond systems ($N_d > 0$), the probability of the flip becomes smaller than 1/2 owing to the distribution of the surrounding decoration spins.

The internal field on the central spin in this configuration is

$$h(n_1, n_2, n_3, n_4) = 2J(N_d - n_1 + n_2 - n_3 - n_4), \quad (25)$$

where n_1 is the number of + spins on the ferromagnetic paths in the antiparallel state of the system spins. Similarly, n_2 is that on the antiferromagnetic paths in the antiparallel state, n_3 is that on the ferromagnetic paths in the parallel state, and n_4 is that on the antiferromagnetic paths in the parallel state.

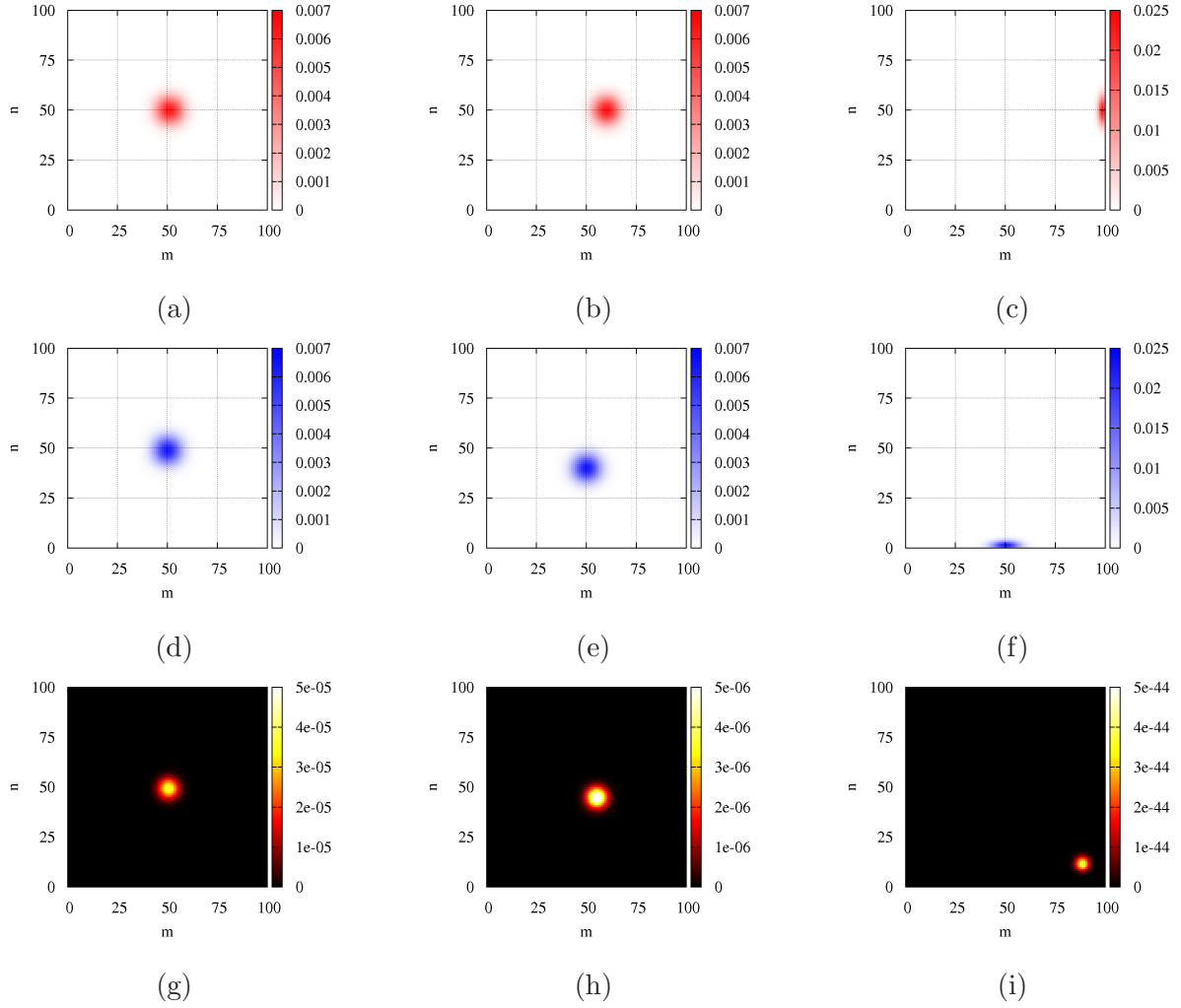


Fig. 4. (Color online) We set the number of decoration spins $N_d = 200$. (Top row) Probability distribution function of parallel state $P_{++}^{(N_d)}(m, n)$ as a function of the numbers of + decoration spins m and n in the cases of (a) $T = 100$, (b) $T = 10$, and (c) $T = 1$. (Middle row) Probability distribution function of antiparallel state $P_{+-}^{(N_d)}(m, n)$ as a function of the numbers of + decoration spins m and n for (d) $T = 100$, (e) $T = 10$, and (f) $T = 1$. (Bottom row) Overlap probability distribution function of parallel state $P_{++}^{(N_d)}(m, n)$ and probability distribution function of antiparallel state $P_{+-}^{(N_d)}(m, n)$ as a function of the numbers of + decoration spins m and n in the case of (g) $T = 100$, (h) $T = 10$, and (i) $T = 1$. Note that the ranges of values are not the same at all temperatures.

In the thermal bath transition probability, the flip probability of the center spin $\mathcal{P}_{\text{flip}}$ is given by

$$\mathcal{P}_{\text{flip}} = \sum_{(n_1, n_2, n_3, n_4)} Q_{+-}^{(2N_d)}(n_1) R_{+-}^{(2N_d)}(n_2) Q_{++}^{(2N_d)}(n_3) R_{++}^{(2N_d)}(n_4) \times \frac{1}{1 + \exp[-2\beta h(n_1, n_2, n_3, n_4)]} \quad (26)$$

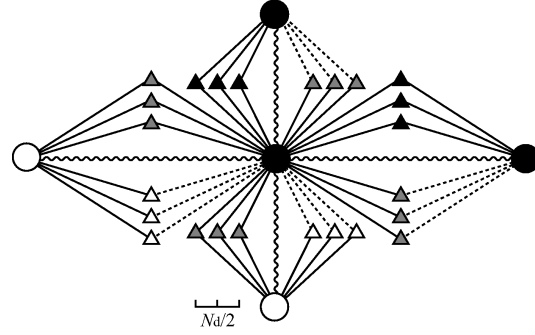


Fig. 5. Central system spin surrounded by two up system spins and two down system spins, which we call a “free spin”. The black, white, and gray symbols denote +, −, and disordered spins, respectively. If decorated bonds are absent, the flip probability of the center system spin is exactly 1/2. However, if decorated bonds exist, the flip probability of the center system spin is less than 1/2 owing to the entropy effect. The number of decoration spins is N_d for each decorated bond.

$$= \frac{1}{(4 \cosh 2\beta J)^{2N_d}} \sum_{(n_1, n_2, n_3, n_4)} \binom{N_d}{n_1} \binom{N_d}{n_2} \binom{N_d}{n_3} \binom{N_d}{n_4} \times \frac{\exp[4\beta J(n_3 - n_2)]}{1 + \exp[-4\beta J(N_d - n_1 + n_2 - n_3 - n_4)]}. \quad (27)$$

Figure 6 shows the dependence of the flip probability of the free spin $\mathcal{P}_{\text{flip}}$ as a function of N_d at $T = 5, 3, 2, 1$, and 0. Here, we find that the stabilization effect is significant when N_d is large at low temperatures.

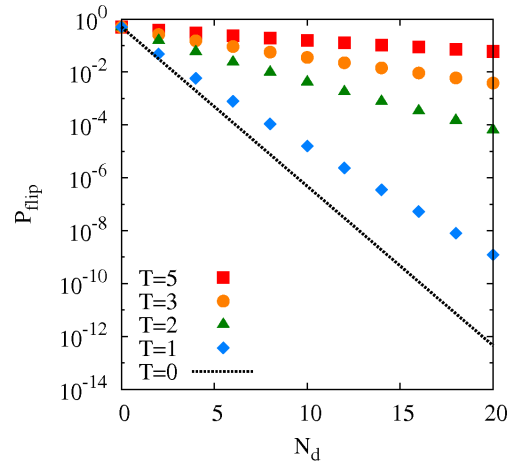


Fig. 6. (Color online) Flip probability of the free spin $\mathcal{P}_{\text{flip}}$ as a function of the number of decoration spins for several temperatures. The squares, circles, triangles, and diamonds denote the data for $T = 5, 3, 2$, and 1, respectively. The low-temperature limit of the probability is shown by the dotted line.

We define the time scale of the evolution by

$$\tau_{\text{eff}} = \mathcal{P}_{\text{flip}}^{-1}. \quad (28)$$

It increases rapidly with N_d . Note that the low-temperature limit of τ_{eff} is finite, because the slowing down is caused by the entropy effect, not by energy. Namely,

$$\lim_{T \rightarrow 0} \mathcal{P}_{\text{flip}} = \frac{1}{2} \left(\frac{1}{4} \right)^{N_d}. \quad (29)$$

This limit is shown by the dotted line in Fig. 6.

4. Monte Carlo Simulation

In the previous section, we calculated the effective time of a flipping spin. We study the relaxation process of system magnetization on the square lattice system shown in Fig. 1(b) at $T = 3$, which is above the critical temperature in this section. We set $N = 20^2$ as the number of system spins. Data are obtained by taking the average over one thousand samples in cases of $N_d = 8, 16, 24, 32$, and 40 . As N_d increases, the relaxation of system magnetization becomes slow. We scale these relaxation processes by the time scale $\tau_{\text{eff}}(N_d)$ (Table I) estimated using eq. (28), and plot them in Fig. 7. All the relaxations of system magnetization converge in a scaling function, which indicates that the analysis in the previous section works well. In the case of $N_d = 200$ shown in Fig. 2, effective relaxation time is estimated to be $\tau_{\text{eff}} \sim 10^{20}$ MCS. Therefore, we see no relaxation within 100 MCS.

Next, we consider the slowing down at the critical temperature and below the critical temperature. In the present model, the critical temperature is $T_c = \frac{1}{2} \log(1 + \sqrt{2})J'$ because the effective coupling is given by $K_{\text{eff}} = \beta J'$. The relaxation curves at the critical temperature obey a power law decay, while those below the critical temperature obey an exponential decay

N_d	8	16	24	32	40
τ_{eff}	1.03037×10^2	3.01700×10^3	7.96926×10^4	2.00850×10^6	4.92665×10^7

(a) $T = 2$

N_d	8	16	24	32	40
τ_{eff}	5.43835×10	8.96284×10^2	1.34004×10^4	1.91522×10^5	2.66641×10^6

(b) $T = T_c$

N_d	8	16	24	32	40
τ_{eff}	1.77064×10	1.08986×10^2	6.17373×10^2	3.36029×10^3	1.78598×10^4

(c) $T = 3$

Table I. Effective relaxation times of the free spin system τ_{eff} at $T = 2$, $T = T_c$, and $T = 3$ as a function of the number of decoration spins N_d .

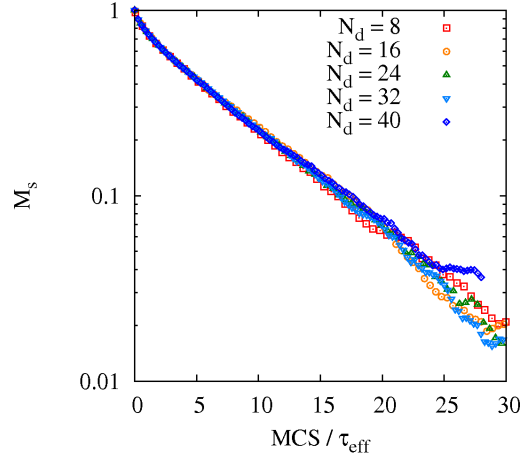


Fig. 7. (Color online) Semilog plot of the relaxation of the system magnetization at $T = 3$ which is above the critical temperature. The squares, circles, triangles, inverted triangles and diamonds denote the case of $N_d = 8, 16, 24, 32$ and 40 , respectively. Relaxation curves obey the exponential function: $M(t) = 0.86e^{-t/7.31}$.

toward spontaneous magnetization. In both cases, we find that the scaling works very well, as shown in Fig. 8. Therefore, we conclude that this mechanism of slowing down works at all temperatures. Both above and below the critical temperature, the relaxation curves can be fitted to the exponential function such as $M_s(t) = Ae^{-t/\tau} + M_{\text{eq}}$. In the case of $T = 3$, we obtain the following parameters: $A = 0.859$ and $\tau = 7.31$ at $M_{\text{eq}} = 0$. In the same way, we obtain the following parameters in the case of $T = 2$: $A = 0.0609$ and $\tau = 1.52$ at $M_{\text{eq}} = 0.911$. On the other hand, at the critical point, the relaxation curve obeys the power law such as $M_s(t) = At^{-b}$. We obtain the following parameters: $A = 0.90$, $b = 0.0569$.

This slowing down mechanism holds the effect of the system spins as well as that in the case of regular system (*i.e.*, with no decoration spins), because the slowing down behavior is just a local effect.

If we set $J' = 0$, then the system is in the complete paramagnetic state, and all the spin configurations of system spins have the same energy. However, because of the entropic slowing down studied above, the system can maintain any configuration for a long time. Thus, we may use such a system as a new type of memory system, which we would call a spin blackboard. If we increase the temperature, we can erase the information of spin configuration.

5. Conclusion

We studied the microscopic mechanism of the increase in the relaxation time of the decorated bond system. We call this slow relaxation phenomenon “entropic slowing down”. The origin of the entropic slowing down is the large number of degenerate configurations due to

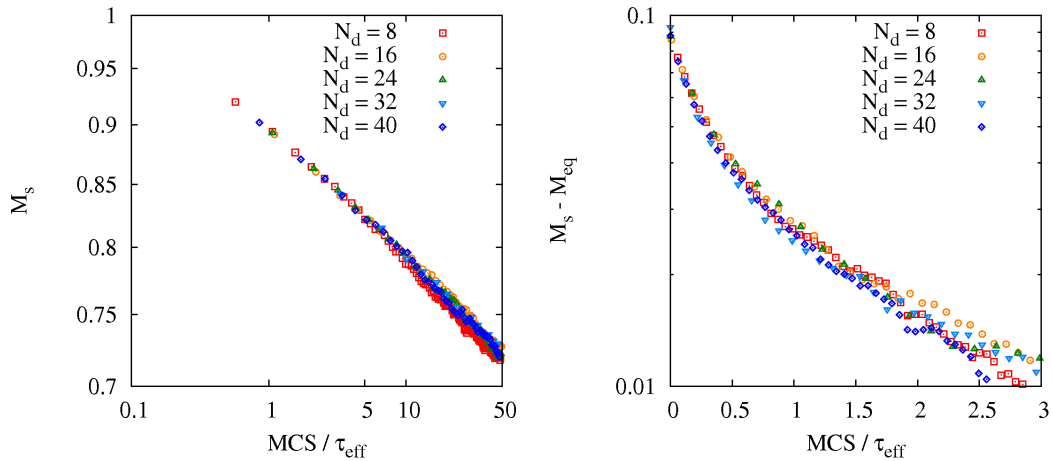


Fig. 8. (Color online) Double logarithmic plot of the relaxation of the system magnetization at $T = T_c$ (left panel) and semilog plot of the difference between system magnetization and the equilibrium value $M(t) - M_{\text{eq}}$ at $T = 2$, which is below the critical temperature (right panel). At $T = 2$, the equilibrium value of magnetization $M_{\text{eq}} = 0.911$. The symbols are the same as those in Fig. 7. Magnetization curves obey the power function $M(t) = 0.90t^{-0.057}$ at the critical point (left panel) and the exponential function $M(t) = 0.061e^{-t/1.52} + 0.911$ at $T = 2$ (right panel).

frustration and not to the energy gap between metastable and stable states. If we set an additional interaction such as J' , the ground state is an ordered state. However, the system cannot reach the ground state because of the freezing effect when it is cooled from a high-temperature disordered state. The system is trapped in some random configuration in a temperature region on the order of J , and no change occurs at low temperatures. Even if there is no additional interaction, this entropic slowing down also appears. We estimated effective relaxation time as a function of temperature and the number of decoration spins analytically. We also studied the relaxation process by a Monte Carlo simulation by the heat bath method. The scaling analysis was successfully performed at all temperatures including the critical temperature.

Originally, the above model with decoration spins has been proposed to explain the slowing down in the system where reentrant phase transition occurs.¹³ We expect that this entropic slowing down also appears in more complicated systems such as spin glass. There, some parts of the random spin system are less frustrated where the spins are strongly correlated, while other parts are highly frustrated where the spins remain disordered. We can interpret the former parts by “system spins” and the latter by “decoration spins”. In this course-grained picture, the spin order can be formed in the network of the former parts.

Moreover, we proposed a new type of memory system, *i.e.* the spin blackboard in which any spin configuration can be stored owing to the entropy effect. If we can prepare a “micelle” type lattice in which a system spin is surrounded by many decoration spins, a spin blackboard

device can be made. We expect that some examples of entropic slowing down will be realized and the spin blackboard behavior will be demonstrated experimentally.

The thermal annealing method^{21,22} is adopted in many problems: it is a very efficient method of obtaining a stable state. However, the thermal annealing method would not be efficient for obtaining the ground state in systems with entropic slowing down. A number of researchers have studied the quantum annealing method²³⁻³⁴ of obtaining the ground state of random systems as a substitute for thermal annealing. We have found that the quantum annealing method is successful in determining the ground state of this entropic slowing down system. The mechanism of this method will be reported elsewhere.

Acknowledgments

The authors would like to express their thanks to Masaki Hirano, Naomichi Hatano and Eric Vincent for helpful discussions. ST also thanks Atsushi Kamimura for the critical reading of this manuscript. This work was partially supported by Research on Priority Areas “Physics of new quantum phases in superclean materials” (Grant No. 17071011) from MEXT, and also by the Next Generation Super Computer Project, Nanoscience Program from MEXT, The authors also thank the Supercomputer Center, Institute for Solid State Physics, University of Tokyo for the use of its facilities.

Appendix: Another Energy Scale: $N_d J$

In this paper, we set the energy unit to be J . In this appendix, we analyze the flip probability $\mathcal{P}_{\text{flip}}$ regarding $N_d J$ as the energy unit because the system spins are surrounded N_d decoration spins. In Fig. A-1 we depict the flip probability of the free spin as a function of the number of decoration spins for the reduced temperature $T/N_d = 0.1J, 0.2J$, and J . At low reduced temperatures, a nonmonotonic behavior appears, which can be understood as follows. The molecular field on a free spin from the outside decoration spins is given by $-JN_d \tanh(2\beta J)$. When $\alpha = T/(N_d J)$ is small, $N_d -JN_d \tanh(2\beta J) \simeq JN_d$ is small and thus molecular field increases with N_d , which causes a decrease in P_{flip} . On the other hand, when $\alpha = T/(N_d J)$ is large, $-JN_d \tanh(2\beta J) \simeq -2J/\alpha$, which does not depend on N_d . For a given T/N_d , the temperature T increases as N_d increases and thus P_{flip} approaches to its high temperature limit $P_{\text{flip}} = 0.5$.

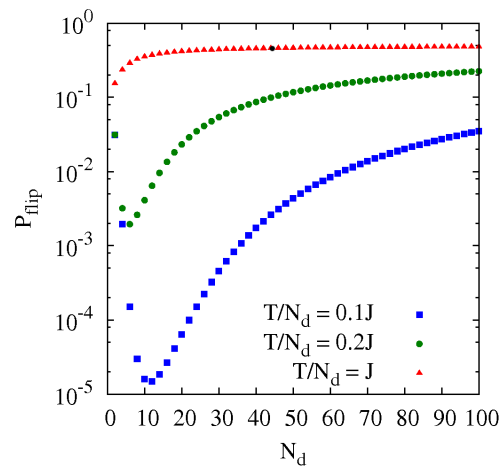


Fig. A.1. (Color online) Flip probability of the free spin \tilde{P}_{flip} as a function of the number of decoration spins at several temperatures. The squares, circles, and triangles denote the data for $T/N_d = 0.1J, 0.2J$, and J , respectively.

References

- 1) K. Kawasaki: Phys. Rev. **145** (1966) 224.
- 2) M. Suzuki and R. Kubo: J. Phys. Soc. Jpn. **24** (1967) 51.
- 3) S. Miyashita and H. Takano: Prog. Theor. Phys. **73** (1985) 1122.
- 4) N. Ito: Physica A **192** (1993) 604.
- 5) D. S. Fisher and D. A. Huse: Phys. Rev. B **38** (1988) 373.
- 6) T. Kawasaki and S. Miyashita: Prog. Theor. Phys. **89** (1993) 985.
- 7) H. Takano and S. Miyashita: J. Phys. Soc. Jpn. **58** (1989) 3871.
- 8) E. Vincent: cond-mat/0603583 and references therein.
- 9) P. Nordblad and P. Svedlindh: in *Spin-Glasses and Random Fields*, ed. A. P. Young (World Scientific, 1998), p. 1, and references therein.
- 10) J. P. Bouchaud, L. F. Cugliandolo, J. Kurchan and M. Mezard: in *Spin-Glasses and Random Fields*, ed. A. P. Young (World Scientific, 1998), p.161, and references therein.
- 11) M. Mezard, G. Parisi and M. A. Virasoro: *Spin Glass Theory and Beyond*, World Scientific, 1987.
- 12) K. H. Fischer and J. A. Hertz: *Spin Glasses*, Cambridge, 1991.
- 13) S. Tanaka and S. Miyashita: Prog. Theor. Phys. Suppl. **157** (2005) 34.
- 14) S. Miyashita and E. Vincent: Eur. Phys. J. B **22** (2001) 203.
- 15) S. Miyashita, S. Tanaka, and M. Hirano: J. Phys. Soc. Jpn. **76** (2007) 083001.
- 16) I. Syozi: Phase Transition and Critical Phenomena, ed. Domb and Green, New York, Academic Press, (1972) vol. 1 and references there in.
- 17) H. Kitatani, S. Miyashita, and M. Suzuki: J. Phys. Soc. Jpn. **55** (1986) 865.
- 18) R. J. Glauber: J. Math. Phys. **4** (1963) 294.
- 19) P. S. Sahní, G. Dee, J. D. Gunton, M. Pahní, J. L. Lebowitz, and M. Kalos: Phys. Rev. B **24** (1981) 410.
- 20) T. Ohta, D. Jasnow, and K. Kawasaki: Phys. Rev. Lett. **49** (1982) 1223.
- 21) S. Kirkpatrick, C. D. Gelatt Jr., and M. P. Vecchi: Science **220** (1983) 671.
- 22) S. Kirkpatrick: J. Stat. Phys. **34** (1984) 975.
- 23) A. B. Finnila, M. A. Gomez, C. Sebenik, C. Stenson and J. D. Doll: Chem. Phys. Lett. **219** (1994) 343.
- 24) T. Kadowaki and H. Nishimori: Phys. Rev. E. **58** (1998) 5355.
- 25) S. Suzuki and M. Okada: J. Phys. Soc. Jpn. **74** (2005) 1649.
- 26) A. Das and B. K. Chakrabarti: *Quantum Annealing and Related Optimization Methods (Lecture Notes in Physics)*, Springer-Verlag, 2005.
- 27) G. E. Santoro and E. Tosatti: J. Phys. A. **39** (2006) R393.
- 28) S. Morita and H. Nishimori: J. Phys. Soc. Jpn. **76** (2007) 064002.
- 29) S. Tanaka and S. Miyashita: J. Magn. Magn. Mat. **310** (2007) e418.
- 30) A. Das and B. K. Chakrabarti: Rev. Mod. Phys. **80** (2008) 1061.
- 31) Y. Matsuda, H. Nishimori, and H. G. Katzgraber: J. Phys. Conf. Ser. **143** (2009) 012003.
- 32) S. Miyashita, S. Tanaka, H. de Raedt, and B. Barbara: J. Phys. Conf. Ser. **143** (2009) 012005.
- 33) K. Kurihara, S. Tanaka, and S. Miyashita: Proceedings of the 25th Conference on Uncertainty in Artificial Intelligence (2009), arXiv:0905.3527.
- 34) I. Sato, K. Kurihara, S. Tanaka, H. Nakagawa, and S. Miyashita: Proceedings of the 25th Confer-

ence on Uncertainty in Artificial Intelligence (2009), arXiv:0905.3528.